Stability Assessment of Isolated Power Systems with High Wind Power Penetration

J. Villena-Lapaz, A. Vigueras-Rodríguez, E. Gómez-Lázaro, I.,
A. Molina-García, J.A. Fuentes-Moreno

***Abstract*—The stability of the electrical systems is a major issue, speccially with the increasing levels of wind penetration. Isolated systems, or systems with weak interconnections with surrounding areas with high amounts of installed wind capacity may experience important stability problems due to the stochastic nature of the wind. The aim of this work is to assess the stability of a power system with high wind penetration level under very high wind conditions. A validated offshore wind farm model, developed by the authors, is used to obtain the wind generated power. Typical models of conventional generation plants have been used to fulfill the system operation requirements.**

I. Introduction

The grid frequency is controlled by conventional power plants. The main goal of this control is to keep the frequency within specified limits depending on each Grid Code. Conventional generators are usually equipped with so-called primary and secondary control, and the inertia of the rotating masses which are synchronously connected to the grid limits the rate of frequency change in case of an imbalance between generated and consumed power. Any power imbalance is catered by the generation by modifying their power input, and the system inertia limits the rate of change of frequency under power imbalances. The lower the system inertia, the higher the rate of frequency change when load or generation variations appear.

System inertia is directly related to the amount of synchronous generators in the power system. This relation is not as obvious when dealing with wind turbine generators due to the electromechanical characteristics of the currently prevailing variable speed technologies, whose turbine speed is decoupled from the grid frequency [1]. In these cases, the inertia contribution of wind turbines is much less than that of conventional power plants [1]–[3]. Besides, some variable speed wind turbines use back-to-back power electronic converters which create an electrical decoupling between the machine and the grid, leading to an even lower participation of wind generation to the system stored kinetic energy.

Some authors suggest that this drawback can be compensated by an adequate implementation of the machine control. In [4], [5] a power reserve is obtained following a power reference value lower than the maximum power which can be extracted from the wind, thus decreasing the turbine power efficiency. References [6], [7], propose a method to let variable-speed wind turbines emulate inertia and support primary frequency control using the kinetic energy stored in the rotating mass of the turbine blades. Reference [7], obtains a power reserve with the help of pitch control when the wind generator works at a close-to-rated power.

On the other hand, fixed–speed wind turbines contribute to the system inertia, releasing the kinetic energy of their rotating mass when the power system frequency is reduced, in a similar way as do synchronous generators [8].

Variable speed wind turbines which are equipped with control loops for emulating inertia or for responding to frequency changes, have a limited time of actuation, since their stored rotational energy decrease very fast when these controls act [9]. After that actions take place, they must lower the setpoint to recover the delivered kinetic energy. When dealing with fixed–speed wind turbines, at wind speeds over the cut out wind, they disconnect, causing a loss in the system inertia. With the increasing levels of wind penetration, this issue might become a major concern.

In this work, the case of a wind farm consisting of fixed–speed wind turbines operating at very high wind speeds, is studied.

II. Model description

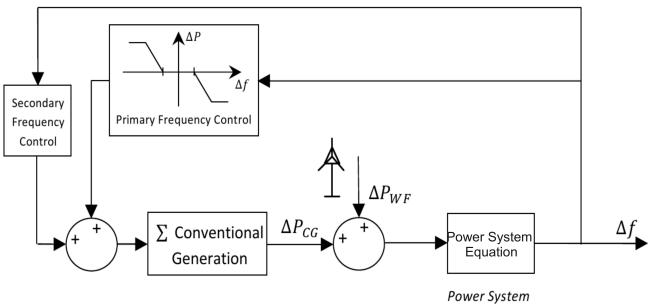

Fig. 1. General Scheme of the power system model.

The generation of the power system model consists of two conventional power plants –thermal and hydroelectric generators– and an offshore wind farm (see Fig. 1), which allows the simulation of different energy mixes.

The authors would like to thank the financial support from "Junta de Comunidades de Castilla-La Mancha" –PII1I09-0273-2610, PEII10-0171-1803– and "Ministerio de Ciencia e Innovación" —ENE2009-13106—

J.E. Villena-Lapaz, E. Gómez-Lázaro, A. Vigueras-Rodríguez are with the Renewable Energy Research Institute, Universidad de Castilla-La Mancha, 02071 Albacete, SPAIN (email: jorgeemilio.villena@uclm.es, antonio.vigueras@uclm.es, emilio.gomez@uclm.es)

A. Molina-García, J.A. Fuentes-Moreno are with the Dept. of Electrical Eng, Technical University of Cartagena, 30202 Cartagena, SPAIN (angel.molina@upct.es, juanalvaro.fuentes@upct.es)

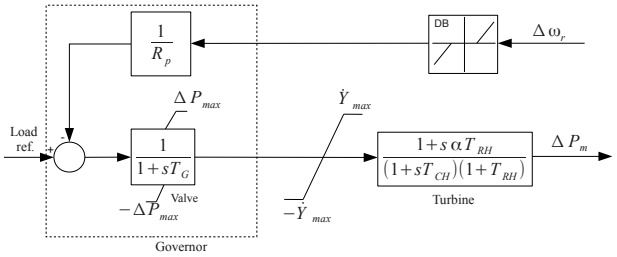

Fig. 2. Model of the thermal–plant

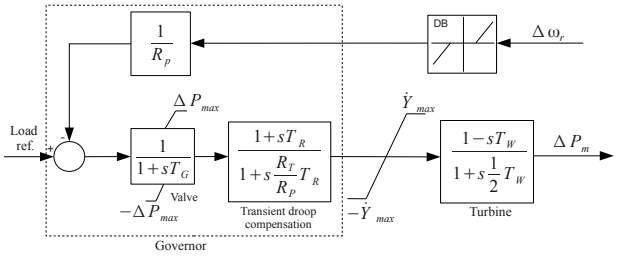

Fig. 3. Model of the hydro–plant

A. Conventional generation

The conventional generation block shown in Fig. 1 consists of a thermal power plant with reheating system and a hydroelectric power plant. These conventional generators have been modeled to participate both in primary and secondary frequency control.

The modeled frequency control of the conventional power plants include the transfer functions for the two main elements of the control loop: the primary energy–mechanical torque converter (governor) and the mechanical torque–electrical power converter (turbine). A transient droop compensation block is also included for the hydro plant model for stability reasons, as detailed in [10], [11].

The block diagrams for the two systems are shown in Fig. 2 and Fig. 3 respectively. The proposed thermal plant consists of a single steam turbine with reheating system. Limitations on slope and maximum power output variations have been included for both generators, as well as a dead band (DB) to model the sensors sensibility and the precision on frequency measuring [12], [13].

B. Wind power production

The wind power production is based on the implementation of an aggregated power fluctuations model of a wind farm developed by some of the authors. This model was previously validated by comparing its results with real power fluctuations measured in Nysted Offshore Wind Farm [14]. For the aim of this work, the wind farm is treated as a single generator with a power curve similar to that shown in Fig. 4 [14]. Due to the shape of that power curve, when reaching the cut out wind speed, around 20 m/s, the disconnection is not sudden. On the contrary, the disconnection for rising wind speeds is progressive.

For this work, fixed–speed wind turbines are considered. For this reason, their contribution to the system inertia is taken into account, as well as their effect over the system frequency when getting disconnected due to high wind speeds.

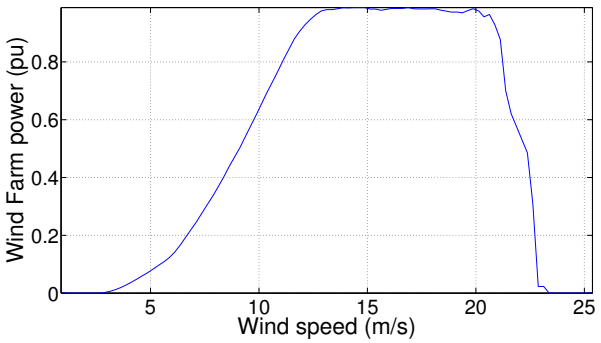

Fig. 4. Aggregated wind farm power curve.

C. Power system description

For stability studies, power systems are usually modeled according to the general scheme shown in Fig. 1. All individual system loads are lumped into an equivalent load with an equivalent damping coefficient (D) [10] and all generators are lumped into a single equivalent rotating mass with a kinetic energy (W_k) that supports power imbalances and which is usually represented by $H = \frac{1/2 J\omega_0^2}{S_{base}}$. In this expression, J is the moment of inertia of the rotating masses coupled to the grid, ω_0 is the rotor nominal speed and S_{base} is the total aparent power of the system. Additionally, frequency deviations (Δf) are used as feedback signals for primary and secondary frequency control.

Under mechanical and electrical disturbances, a rotating machine is subjected to differences in mechanical and electrical torques, T_{mec} and T_{elec}, causing it to change its rotational kinetic energy. Writing $P = \omega T$, and expressing the variables as the sum of the steady state value and the deviation term, $T = T_0 + \Delta T$, $\omega = \omega_0 + \Delta\omega$ and $P = P_0 + \Delta P$, the resulting power balance equation can be written as [10], [15]:

$$\Delta P_{mec} - \Delta P_{elec} = \frac{dW_k}{dt}, \tag{1}$$

which means that any power imbalance between the mechanichal and the electrical power causes a variation in the kinetic energy of the masses which are connected to the grid.

Loads on a power system include a great variety of electrical devices that may or not be affected by changes in system frequency. ΔP_{elec} can be then given by:

$$\Delta P_{elec} = \Delta P_L + D\Delta\omega, \tag{2}$$

where ΔP_L is the non-frequency-sensitive load change and $D\Delta\omega$ is the frequency-sensitive load change. The damping coefficient, D, models the variation in the electric power consumption with respect to speed changes.

In this study ΔP_L is not considered, thus the frequency excursions are exclusively due to fluctuations in wind power generation.

Substituting eq.(2) in (1) and dividing by S_{base} follows:

$$\frac{\Delta P_{mec}}{S_{base}} = \frac{D\omega_o\Delta\omega}{S_{base}\omega_o} + \frac{1}{S_{base}}\frac{dW_k}{dt},$$

where those terms which depend on ω have been multiplied and divided by $\omega_o = \omega_{base}$ in order to work with speeds also in pu. Finally, introducing $D' = \frac{D\omega_o}{S_{base}}$ and taking into account that in pu ω is equal to f, yields the following pu equation:

$$\Delta P_{mec,pu} = D'\Delta f + \frac{1}{S_{base}}\frac{dW_k}{dt}. \quad (3)$$

The term $W_k = \frac{1}{2}J\omega^2$ is the sum of the kinetic energy of the convencional generators and of the wind farm.

$$W_k = \frac{1}{2}J_{conv}\omega^2 + \frac{1}{2}J_{WF}\omega^2 \quad (4)$$

Both conventional generators keep connected during the simulations. Therefore, their kinetic energy depends only on the rotational speed, w. In other words, the moment of inertia of the conventional generators , J_{conv}, remains constant during the simulations. On the other hand, the wind farm is operating at its rated speed, with an average wind speed which is near or even over the cut out speed (see 4). It means that, at some point, some of the turbines will be disconnected, while others will remain on. As a consequence, the amount of rotors connected to the grid will decrease, and so will the moment of inertia of the wind farm, J_{WF}. If J^0_{WF} is the moment of inertia of the wind farm when all the turbines are connected, i.e. when $P_{WF} = 1$ pu, and $J_{WF} = 0$ when all of them are disconnected due to a very high wind speed, i.e. $P_{WF} = 0$, it is possible to define a variable moment of inertia of the wind farm as

$$J_{WF}(t) = J^0_{WF} \cdot P_{WF}(t), \quad (5)$$

where $P_{WF}(t)$ is the wind farm power production, explained in subsection II-B.

Using expression 4, it is possible to write the last term in eq 3 as follows:

$$\begin{aligned}\frac{1}{S_{base}}\frac{dW_k}{dt} &= \frac{1}{2S_{base}}\frac{d}{dt}((J_{conv}+J_{WF})\omega^2) = \\ &= \frac{1}{2S_{base}}J_{conv}\frac{d\omega^2}{dt} + \\ &+ \frac{1}{2S_{base}}J_{WF}\frac{d\omega^2}{dt} + \\ &+ \frac{1}{2S_{base}}\omega^2\frac{dJ_{WF}}{dt}\end{aligned} \quad (6)$$

For a level of wind penetration given by $L_p = \frac{S_{WF}}{S_{base}}$, being S_{WF} the installed wind capacity, the amount of installed conventional power can be expressed as

$$\begin{aligned}S_{WF} &= L_p S_{base} \\ S_{conv} &= (1-L_p)S_{base}\end{aligned}$$

since $S_{base} = S_{conv} + S_{WF}$.

Writing $\omega = \omega_0 + \Delta\omega$, and neglecting second$-$order terms involving $\Delta\omega$,

$$\frac{d\omega^2}{dt} \approx 2\omega_0\frac{d\Delta\omega}{dt} = 2\omega_0^2\frac{d\Delta f}{dt},$$

with, again, f in pu; and hence,

$$\frac{1}{2S_{base}}J_{conv}\frac{d\omega^2}{dt} = 2H_{conv}(1-L_p)\frac{d\Delta f}{dt}, \quad (7)$$

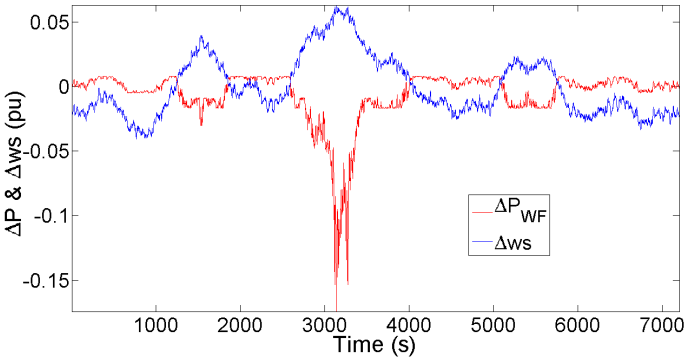

Fig. 5. Wind Farm Power and average wind speed in 2-hour time interval, expressed in per unit

$$\frac{1}{2S_{base}}J_{WF}\frac{d\omega^2}{dt} = 2H_{WF}P_{WF}(t)L_p\frac{d\Delta f}{dt}, \quad (8)$$

$$\frac{1}{2S_{base}}\omega^2\frac{dJ_{WF}}{dt} = H_{WF}L_p f^2\frac{dP_{WF}}{dt}. \quad (9)$$

where H_{conv} and H_{WF} are the inertia constants of the conventional generators and the wind turbines, respectively.

Similarly, the equivalent system inertia H can be calculated as:

$$H(t) = H_{conv}(1-L_p)f^2 + H^0_{WF}L_pP_{WF}(t)f^2 \quad (10)$$

This inertia is not constant, since depends on the number of connected wind turbines, through $H^0_{WF}L_pP_{WF}(t)$.

III. Simulation and Results

Integrating equation 6 into equation 3 the mathematical model proposed for the system is implemented in MATLAB/Simulink to carry out the simulations. The only input to the system is a series of wind power, whose fluctuations produce frequency excursions.

A mix of two conventional power plants (a thermal and a hydro units) and a wind farm has been considered.

The simulated wind farm is located offshore, and consists of 506 MW spread over 10 rows with 22, 2.3 MW fixed–speed wind turbines each. The distance between columns is about 500 m, whereas rows are separated around 900 m. Several 2-hour time intervals of supply power have been simulated for the proposed wind farm. One of these data series has been used for the aim of the study. The selected data series is relevant as it represents a period with average high wind speed of 20 m/s (cut out wind speed), producing disconnections of wind turbines when rising upon that value. These disconnections will cause frequency excursions and, at the same time, the loss of kinetic energy necessary for keeping the system balance. This series, together with the average wind speed (Δws) over the wind farm are shown in Fig. 5, in pu and relative to the initial value, which is considered as the reference value. As can be seen, the average wind speed within the simulation is 1 pu, i.e. 20 m/s. It means that the selected series represents a period of time in which the wind farm is operating in the flat part of its power curve, and when the wind speed rises over 20 m/s, in the cut out zone –see Fig 4. From the abovementioned data

series, only the interval between $t = 2400$ s and $t = 4000$ s has been used. At the beginning of this interval the wind speed and the power production are at the rated levels, and at some point, the wind speed rises, causing an important fall of the power production.

For the inertia constant of the wind turbines, different values can be found in the bibliography. For instance, in [11], a value of $H_{WF} = 5,19$ s is used for big wind turbines, similar to that modeled in this work. In [6] it is estimated a value of 6 s. Three different values are used here: 5, 4 and 3 seconds. With this assumption, three cases are considered in order to assess the influence of it on the system stability.

As mentioned above, the only input to the system is the wind data series, hence the conventional plants have been modeled to produce the difference between the wind power and the load, plus their participation in primary and secondary control.

The values of all parameters of the conventional power plant models used in this work are given in Table I and are obtained from [10], see Figs. 2 and 3. The selected inertia constants of thermal and hydro plants are $H_{thermal} = 4$ s and $H_{hydro} = 3$ s, respectively.

TABLE I
PARAMETERS FOR THE CONVENTIONAL GENERATORS MODELS

Parameter	Thermal plant	Hydro plant
DB	$\pm$20 mHz	$\pm$20 mHz
R_P	5 %	5 %
ΔP_{max}	0.05 pu	0.05 pu
$\dot{Y}_{max}$	0.05 pu/s	0.16 pu/s
$\dot{Y}_{min}$	-0.1 pu/s	-0.16 pu/s
α	0.3 pu	–
T_{RH}	7 s	–
T_{CH}	0.3 s	–
T_w	–	1 s
R_T	–	0.38 pu
H	4 s	3 s

For a given wind data series, several simulations have been carried out for different amounts of loads fed by the generators, i.e. for different level of wind power penetration, and for $H_{WF} = 5$, 4 and 3 s. Starting with a 1,2 GW system, its size is reduced in 100 MW steps to 700 MW. As the wind power rises in relation to the total power, any disconnection of wind turbines has a deeper impact. Eventually instability appears. Some results of the simulations are depicted in figures from 6 to 17. The figures show the frequency excursions (Δf) and the variations of generated power (ΔP) –the conventional generators are shown as one–, as well as the wind speed variation (Δws), on the one hand, and on the other hand, the evolution of the system inertia ($H(t)$, in seconds), for different values of S_{base} (1200 and 700 MW) and of H_{WF}.

The first observation worth pointing out is that when the wind turbines start disconnecting, the term $\frac{dP_{WF}}{dt}$ in equation 9 outputs a very high signal, meaning a sudden change in the system frequency. This is common for all the simulations. Anyway, for the case of $H_{WF} = 3$ s, an unestability that the control systems are not able to restore appears, and remains during the rest of the simulation. This instability disappears when lowering the wind penetration –see figure 14

By comparing the simulations for $S_{base} = 1200$ MW it is remarkable that, the higher the Wind Farm inertia constant considered, the lower the stability. In this way, the maximum frequency excursions observed in figure 6, for $H_{WF} = 5$, s are higher than the other ones. It means that the system gets more sensitive to losses in generation when the wind penetration level rises.

For a certain value of H_{WF}, when augmenting the wind penetration level –by reducing S_{base}–, the instability rises as well, and the oscillations of Δf and ΔP_{conv} get more important.

Figures related to the evolution of the system inertia show how the disconnection of wind turbines produces important losses of kinetic energy, which may cause stability problems. For instance, in Fig. 17, a critical fall of the system inertia under 2,2 s produces the instability which is observed in Fig. 16.

When considering $H_{WF} = 5$ s, being this value higher than that of the conventional generators, a rise in the wind penetration level, i.e, a rise in the proportion of wind turbines relative to the conventional generators, implies a rise of the system inertia as well. For the case of $H_{WF} = 3$ s, the effect is the opposite: the higher the proportion of wind turbines in the system, the less the system inertia –see figures 7 and 9, and 15 and 17–.

IV. CONCLUSIONS

In this work, a variation of the torque balance equation for assessing the stability of a power system with high wind power penetration is proposed. Classical primary energy input control in steam and hydro turbines are also considered to model the power system. An offshore wind farm compound by 10 rows with 22 wind turbines each one is considered as renewable power supply. An aggregated model previously proposed and assessed by the authors is suggested to simulate power fluctuations. In this way, a wind power data series is used to simulate the behaviour of the wind farm when operating at high wind speeds, with the consequent disconnection of wind turbines and the loss of system inertia.

It is shown how, at high levels of wind penetration, especially isolated power systems may experience critical losses of inertia within normal operating conditions, under high winds. It is shown also that, at higher levels of wind penetration the system becomes weaker against eventual wind turbines disconnections due to high winds.

This problem may arise when future wind turbines incorporate frequency response control systems such as inertia emulation, in order to participate in the system stability, as their contribution is limited to some seconds.

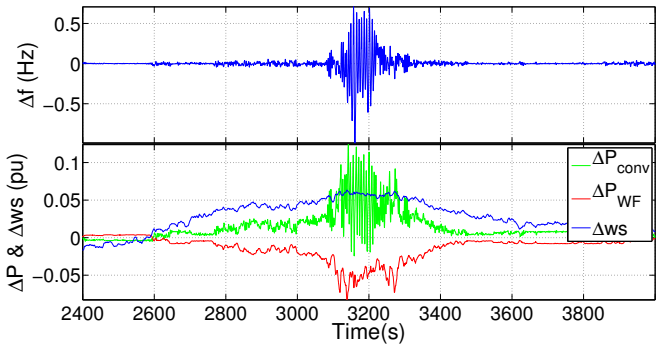

Fig. 6. Frequency excursions, Power generation changes and wind speed during the simulation. $H_{WF} = 5$ s & $S_{base} = 1200$ MW

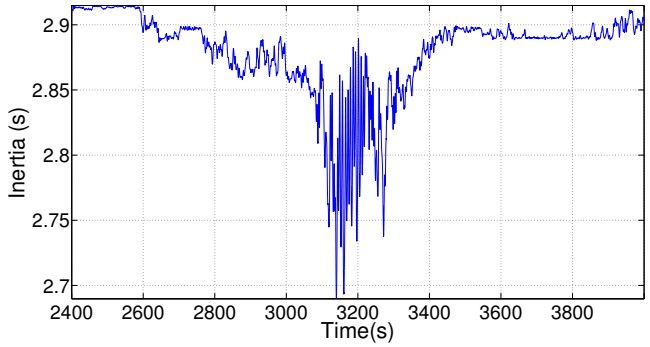

Fig. 7. Evolution of the system inertia during the simulation. $H_{WF} = 5$ s & $S_{base} = 1200$ MW

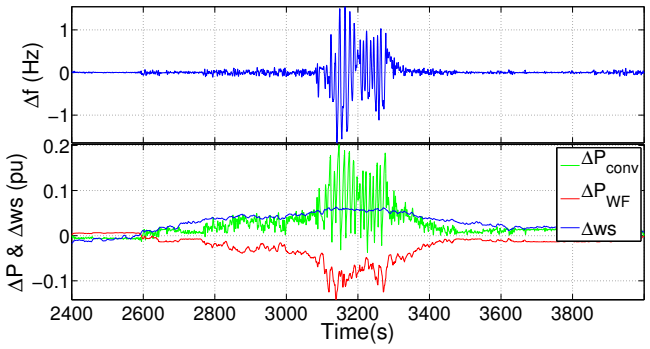

Fig. 8. Frequency excursions, Power generation changes and wind speed during the simulation. $H_{WF} = 5$ s & $S_{base} = 700$ MW

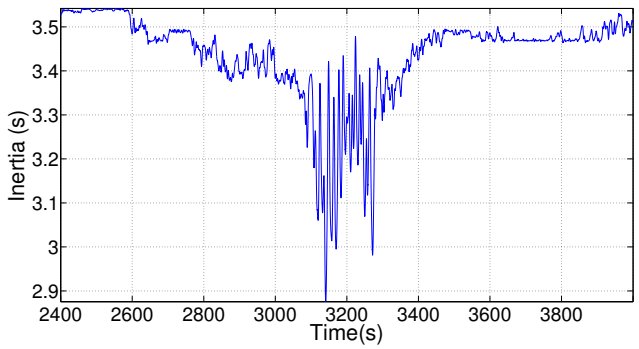

Fig. 9. Evolution of the system inertia during the simulation. $H_{WF} = 5$ s & $S_{base} = 700$ MW

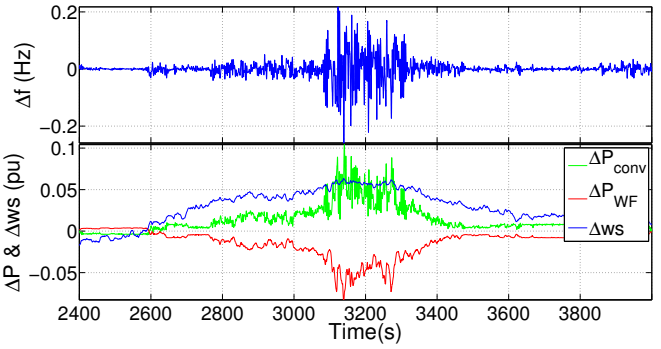

Fig. 10. Frequency excursions, Power generation changes and wind speed during the simulation. $H_{WF} = 4$ s & $S_{base} = 1200$ MW

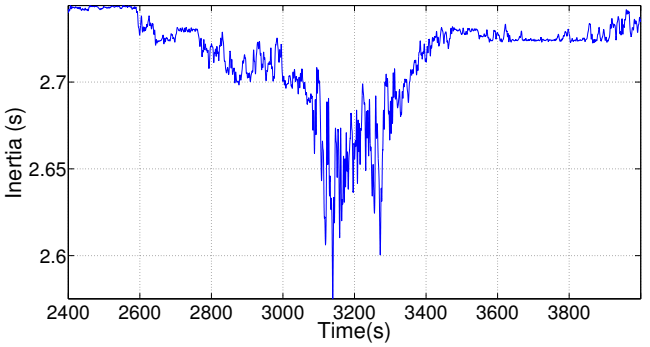

Fig. 11. Evolution of the system inertia during the simulation. $H_{WF} = 4$ s & $S_{base} = 1200$ MW

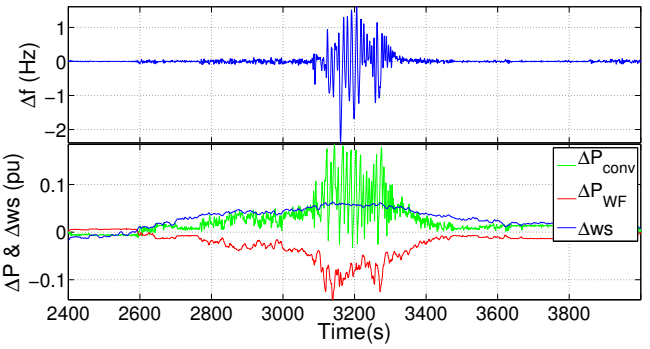

Fig. 12. Frequency excursions, Power generation changes and wind speed during the simulation. $H_{WF} = 4$ s & $S_{base} = 700$ MW

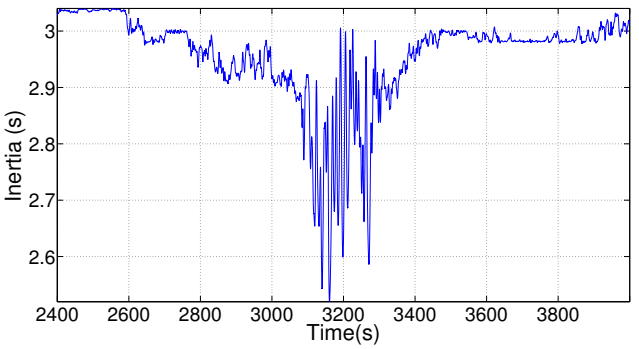

Fig. 13. Evolution of the system inertia during the simulation. $H_{WF} = 4$ s & $S_{base} = 700$ MW

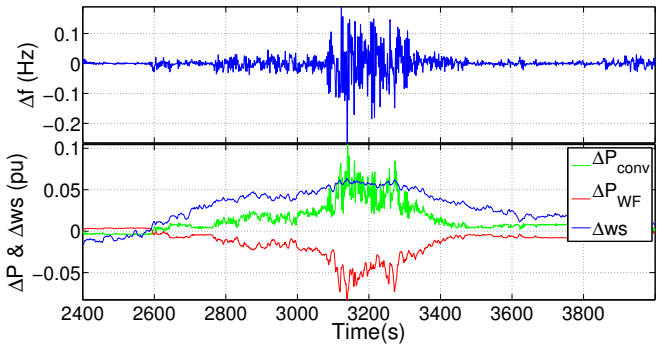

Fig. 14. Frequency excursions, Power generation changes and wind speed during the simulation. $H_{WF} = 3$ s & $S_{base} = 1200$ MW

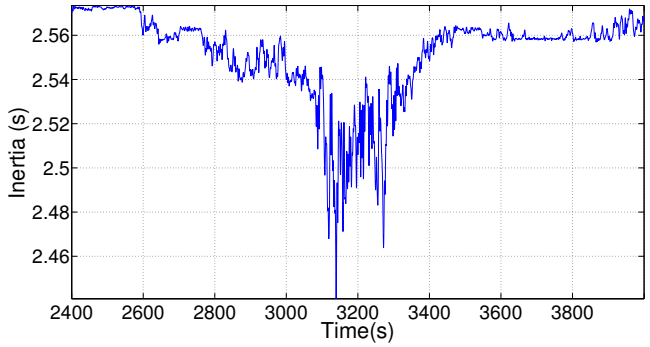

Fig. 15. Evolution of the system inertia during the simulation. $H_{WF} = 3$ s & $S_{base} = 1200$ MW

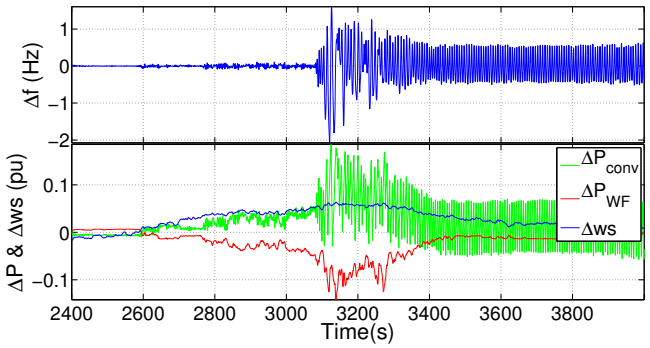

Fig. 16. Frequency excursions, Power generation changes and wind speed during the simulation. $H_{WF} = 3$ s & $S_{base} = 700$ MW

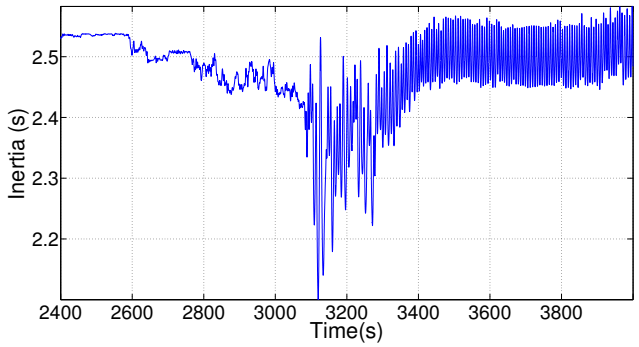

Fig. 17. Evolution of the system inertia during the simulation. $H_{WF} = 3$ s & $S_{base} = 700$ MW

REFERENCES

[1] G. Lalor, A. Mullane, and M. O'Malley, "Frequency control and wind turbine technologies," *IEEE Transactions on Power Systems*, vol. 20, pp. 1905–1913, 2005.

[2] G. Lalor, J. Ritchie, S. Rourke, D. Flynn, and M. J. O'Malley, "Dynamic frequency control with increasing wind generation," in *Proc. IEEE Power Engineering Society General Meeting*, 2004, pp. 1715–1720.

[3] A. Mullane and M. O'Malley, "The inertial response of induction-machine-based wind turbines," *IEEE Transactions on Power Systems*, vol. 20, no. 3, pp. 1496–1503, 2005.

[4] P. Soerensen, A. D. Hansen, K. Thomsen, H. Madsen, H. A. Nielsen, N. K. Poulsen, F. Iov, F. Blaabjerg, and M. H. Donovan, "Wind farm controllers with grid support," *5th Int. Workshop Large-Scale Integration Wind Power Transmission Networks Offshore Wind Farms*, 2005.

[5] M. E. Mokadem, V. Courtecuisse, C. Saudemont, B. Robyns, and J. Deuse, "Experimental study of variable speed wind generator contribution to primary frequency control," 2008.

[6] J. Morren, S. W. H. de Haan, W. L. Kling, and J. A. Ferreira, "Wind turbines emulating inertia and supporting primary frequency control," *IEEE Transactions on Power Systems*, vol. 21, no. 1, pp. 433–434, 2006.

[7] P. Bousseau, R. Belhomme, E. Monnot, N. Laverdure, D. Boeda, D. Roye, and S. Bacha, "Contribution of wind farms to ancillary services," *CIGRE*, 2006.

[8] J. Ekanayake and N. Jenkins, "Comparison of the response of doubly fed and fixed-speed induction generator wind turbines to changes in network frequency," *IEEE Transactions on Energy Conversion*, vol. 19, no. 4, pp. 800–802, 2004.

[9] G. Tarnowski, P. Kjar, P. Sorensen, and J. Ostergaard, "Variable speed wind turbines capability for temporary over-production," in *Power Energy Society General Meeting, 2009. PES '09. IEEE*, july 2009, pp. 1 –7.

[10] P. Kundur, *Power System Stability and Control*. McGraw-Hill, 1994.

[11] N. R. Ullah, T. Thiringer, and D. Karlsson, "Temporary primary frequency control support by variable speed wind turbines— potential and applications," *IEEE Transactions on Power Systems*, vol. 23, no. 2, pp. 601–612, 2008.

[12] REE, "P.o. 7.1. servicio complementario de regulacin primaria," REE, http://www.ree.es, Tech. Rep., August 1998 — available on-line.

[13] "UCTE Operation Handbook – ver. 2.5," UCTE, http://www.ucte.org, Tech. Rep., July 2004 — available on-line.

[14] A. Vigueras-Rodriguez, P. Srensen, N. Cutululis, A. Viedma, and M. Donovan, "Wind model for low frequency power fluctuations in offshore wind farms," *Wind Energy*, vol. 13, pp. 471–482, 2010.

[15] A. Wood and B. Wollenberg, *Power Generation, Operation and Control*. J. Wiley & sons, 1996.